ChemPubSoc Europe

DOI: 10.1002/slct.201801590

Chemistry SELECT Full Papers

Organic & Supramolecular Chemistry

Unsubstituted Oxacalix[*n*]arenes (*n* = 4 and 8): A Conformational Study in Solution and Solid State and Interaction Studies with Aromatic Guests

Anna Peterson,[a, b] Sandra Kaabel,[b] Iiris Kahn,[b] Tõnis Pehk,[a] Riina Aav,*[b] and Jasper Adamson*[a]

We present single crystal structures of unsubstituted oxacalix[4]arene and oxacalix[8]arene macrocycles and investigate the weak supramolecular interactions that govern their packing in the solid state. We further show that the unsubstituted oxacalix[4]arene shows weak complexation with two aromatic guest species, benzoic acid and ferrocene, in $CDCl_3$, whereas the oxacalix[8]arene host does not complex with these guest molecules. We also present NMR titration experiments with non-aromatic acids and DFT calculations that signify the importance of π-π interactions for complexation with benzoic acid. Weak complexation is also observed between electron-rich aromatic guest molecules and the unsubstituted oxacalix[4]arene host.

Introduction

Macrocycles are cyclic oligomers that are widely investigated in modern supramolecular science due to their broad capacity for molecular recognition. A number of families of macrocycles, e.g., crown ethers,[1,2] cyclodextrins,[3] cucurbiturils,[4,5] and calix[*n*]arenes[6,7] are well-established and their host-guest complexation properties well-investigated.

Although oxacalix[n]arenes or oxa[1*n*]metacyclophanes are formally related to the third generation of synthetic receptors of calix[*n*]arenes, these potential host compounds are comparatively much less investigated.[8] In the structures of oxacalix[*n*]arenes, oxygen-bridges replace the methylene linkages between aromatic linkers that results in macrocycles combining the key features of crown ethers and calix[*n*]arenes. Therefore, oxacalix[*n*]arenes have unique cavity sizes and shapes as well as capability for both hydrogen-bonding and π-π interactions.

In fact, the first of these compounds was discovered in 1966, however, isolation of pure substances was challenged by poor synthetic yields and solubility of the products.[9] Interest in oxacalix[*n*]arenes was revived in 2005 when Katz and coworkers realized the great potential of nucleophilic aromatic substitution (S_NAr) protocols for the synthesis of a number of nitro-substituted oxacalix[4]arenes in high yields.[10] Since then, other research groups have complemented the library of oxacalix[*n*]arenes by utilizing various aromatic linkers,[11,12] substituents (e.g., aliphatic,[13] amine,[14] halide[15] groups) and introducing larger odd- and even-numbered oxacalix[*n*]arenes (*n* = 5–8).[16,17] The emerging subclass of oxacalix[*n*]arenes that incorporates heterocyclic aromatic linkers is known as oxacalix[*n*]hetarenes.[8]

Despite the synthetic endeavors in the field, host-guest recognition properties of oxacalix[*n*]arenes remain poorly understood and have a primary focus on substituted oxacalix[4]arenes or oxacalix[4]hetarenes. Specific examples include the work by Katz and coworkers who studied *o*-salicylic acid complexation with oxacalix[4]naphthalene[2]naphthyridine[11] and by Shimizu et al. who showed ferrocene and its oxidized form ferrocenium to complex with nitro-substituted oxacalix[4]arenes.[18] In 2015, the group of Gattuso showed polycationic oxacalix[4]arenes to complex with paraquat and neutral aromatic guests in aqueous media.[19,20]

Another class of macrocycles that are comparable with oxacalix[4]arenes are unsubstituted or dehydroxylated calix[4]arenes that have capacity for π-π interactions alone.[21] Investigation of such macrocycles started with the work of Biali and coworkers,[22] however, to the best of our knowledge, their host-guest complexation studies are also relatively scarce.[23]

In this work, we prepared oxacalix[4]arene (**1a**) and oxacalix[8]arene (**1b**) (Figure 1) hosts based on the fragment-coupling synthesis procedure, published originally by Zhou et al.,[24] to explore their conformation in solution and solid state and to determine their complexation properties in comparison to other oxacalix[*n*]arenes and oxacalix[*n*]hetarenes. Herein, we present, for the first time, the crystal structures of **1a** and **1b**, together with a study of the weak supramolecular forces directing the aggregation of these molecules in the solid state. Furthermore, we describe the complexation properties of **1a** and **1b** with aromatic guest molecules, which indicates the strength of complexation of the "naked" oxacalix[*n*]arene scaffold.

[a] *A. Peterson, Prof. T. Pehk, Dr. J. Adamson*
Chemical Physics Laboratory, National Institute of Chemical Physics and Biophysics, Akadeemia tee 23, 12618, Tallinn, Estonia
E-mail: jasper.adamson@kbfi.ee

[b] *A. Peterson, S. Kaabel, Dr. I. Kahn, Prof. R. Aav*
Department of Chemistry and Biotechnology, Tallinn University of Technology, Akadeemia tee 15, 12618 Tallinn, Estonia
E-mail: riina.aav@ttu.ee

Supporting information for this article is available on the WWW under https://doi.org/10.1002/slct.201801590

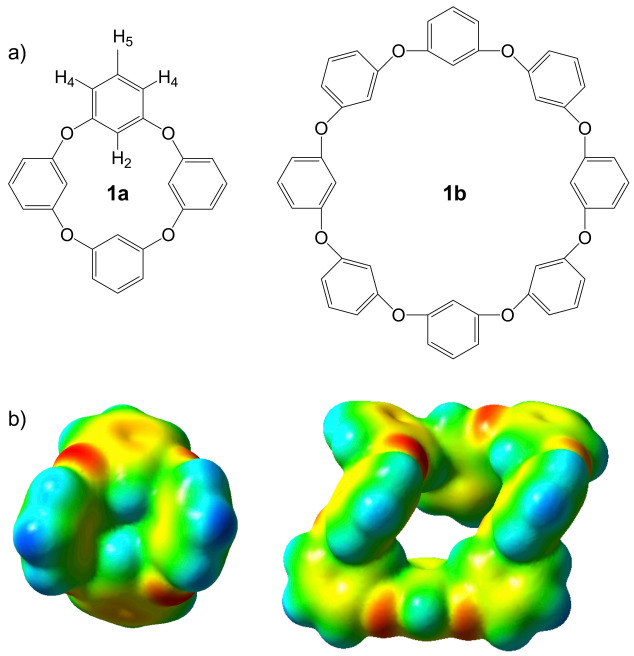

Figure 1. a) Structure of oxacalix[4]arene (**1 a**) with indication of proton numbers and oxacalix[8]arene (**1 b**) investigated in this work. b) molecular electrostatic potential images for **1 a** and for **1 b** as visualized by GaussView 5.0.8.

Results and Discussion

Crystal structures of 1 a and 1 b

Two polymorphs of the compound **1 a** were obtained, one in a centrosymmetric space group *C*2/*c*, with half of the macrocycle in the asymmetric unit and second in a polar non-centrosymmetric space group $P-42_1c$ with one quarter of **1 a** in the asymmetric unit; see Supporting information (SI) for crystallographic details. Overlay of the oxacalix[4]arene molecules in polymorphs I and II shows that the conformation of **1 a** changes very little between the two crystal structures (Figure S1), indicating that the polymorphism of these structures does not root from conformational differences, but is rather the result of differences in crystal packing.

Dominant intermolecular interactions within the crystal structures of the two polymorphs of **1 a** were explored by the whole-molecule approach of energy framework analysis[25,26] using the *CrystalExplorer*[27] software (See SI for details), together with a more detailed look on specific intermolecular contacts. Packing of the macrocycles is mainly directed by off-center aromatic-aromatic interactions, known for electron-rich aromatic systems,[28] and multiple weak C−H···O hydrogen bonds. Oxacalix[4]arene adopts a 1,3-alternate saddle-shaped conformation in the crystal structures, which leads to a columnar stacking of **1 a** in both of the polymorphs (Figure 2c). Based on the calculated energy frameworks the stacking forces are the dominant intermolecular interactions in both polymorphs (Figure 2a, b). Interaction energies between nearest neighboring molecules in the two polymorphic structures are included in the Supporting Information (Table S1 and S2)

Discrepancies in the packing of the two polymorphs I and II becomes evident when comparing the hydrogen bonding motifs in the respective crystal structures. In polymorph I, four outgoing hydrogen bonds, C6−H6···O1^{i} (d(H···O) = 2.573 Å), and its symmetry equivalents, connect **1 a** into wavy ribbons along the crystallographic *c* axis (Figure 2c), which are further interconnected through a ladder arrangement of four outgoing hydrogen bonds: C9−H9···O2^{ii} (d(H···O) = 2.690 Å) and its symmetry equivalents (Figure 2d). In the oriented non-centrosymmetric crystal structure of polymorph II, eight outgoing hydrogen bonds, C4−H4···O1^{i} (d(H···O) = 2.646 Å) and its symmetry equivalents, connect the columnar stacks of **1 a** in helical motifs along the crystallographic axis *c* (Figure 2e).

The compound **1 b** crystallized in space group $P2_1/c$, with the whole molecule of **1 b** in the asymmetric unit. Weak C–H**...**O hydrogen bonds and π-π stacking appear to direct the supramolecular aggregation of this crystal structure. Two molecules of **1 b**, connected through four hydrogen bonds C2C−H2C···O1F^{i} (d(H···O) = 2.677 Å), C6E−H6E···O1A^{i} (d(H···O) = 2.414 Å) and their symmetry equivalents, form a dimer, in

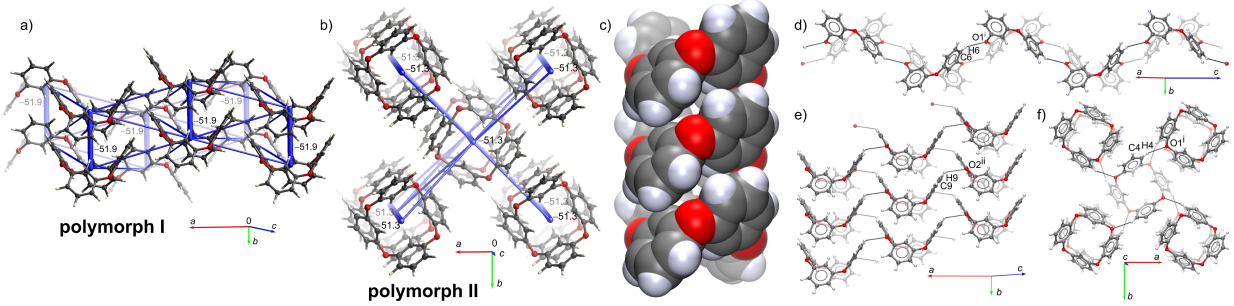

Figure 2. Energy-framework diagrams for the polymorphs I a) and II b) of **1 a** (CCDC 1836367 and 1836368 respectively), showing the total energy E_{tot} in blue cylinders, whose thickness represents the relative strength of molecular packing in different directions within the crystal structure. Both diagrams use a scale factor of 50 and a threshold of 5 kJ mol^{-1}. The E_{tot} contribution from the stacking interaction is indicated on the figures.[27] c) The CPK visualisation of the columnar stacking of **1 a**. Ribbon d) and ladder e) hydrogen bonding motifs in polymorph I of **1 a**. Symmetry codes: i) 1 − x, − y, 1 − z; ii) 1/2 − x, − 1/2 + y, 1.5 − z. f) Helical arrangement of the eight outgoing hydrogen bonds in the polymorph II. Symmetry code: i) $^{1}/_{2}+x$, $^{1}/_{2}-y$, $^{1}/_{2}-z$. Colour codes: C grey, O red and H white. The C–H···O hydrogen bonds d(C–H···O) ≤ Σr(vdW)[H, O] are drawn in black stippled lines.

which four aromatic rings are arranged parallel, indicative of off-center π-π interactions (Figure 3c, d). These dimers are

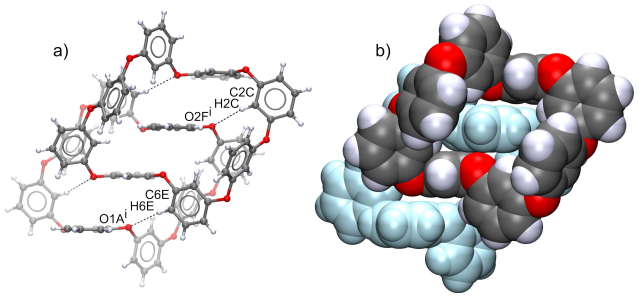

Figure 3. a) Dimeric units in the crystal structure of **1 b**, interconnected through four C–H...O hydrogen bonds and off-centre aromatic-aromatic stacking. b) CPK visualisation of the tight packing of the **1 b** molecules in the dimer. Symmetry code: 1 − x, 1 − y, 1 − z. The C–H···O hydrogen bonds d (C–H···O) ≤ Σr(vdW)[H, O] are drawn in black stippled lines.

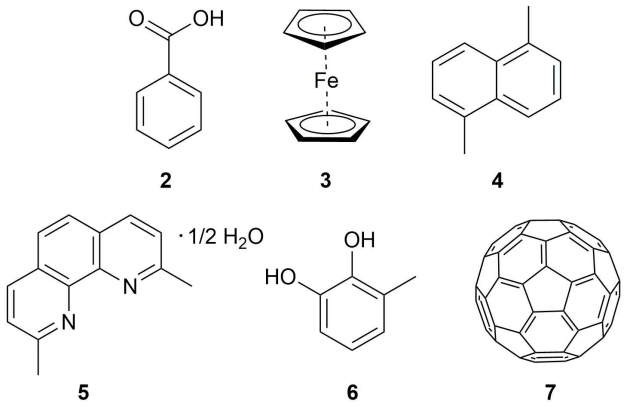

Figure 4. Guest molecules studied for complexation in this investigation.

further packed tightly side-by-side, so that the resulting crystal structure contains no voids (determined using probe radius 1 Å).

Conformations of 1 a and 1 b in solution

For an investigation of the conformations of **1 a** and **1 b** in solution, we performed variable temperature solution ^{1}H NMR and ^{13}C NMR experiments on **1 a** and **1 b** in $CDCl_3$. No line broadening was seen in the temperature region 230–288 K (Figure S11), evidencing that either the structures are in a static conformation in solution or alternatively the rate of exchange between different conformations is so fast on the NMR time scale that no significant line broadening is seen at these temperatures for either macrocycle. Such observations have been made by other researchers for previous studies of substituted oxacalix[4]arenes and oxacalix[4]hetarenes.[10,29,30]

Moreover, we observe an upfield shift for the H_2 and C_2 proton and carbon resonances upon cooling. These proton and carbon atoms point towards the inner cavity of **1a** and **1b**, and this result is in agreement with previous studies that suggest that these upfield shifts could originate from some degree of reorientation of the atoms in the anisotropic shielding cone of adjacent aromatic groups and indicate that similarly to other oxacalix[4]arenes and oxacalix[4]hetarenes, conformations of **1a** and **1b** in solution might resemble their static conformations in the solid state.[8]

Complexation in solution (NMR titrations)

Our following pursuit was to investigate complexation properties of **1 a** and **1 b** with a set of aromatic guest molecules in solution state (Figure 4). All the selected guest species have potential to form π-π interactions with **1 a** and **1 b**, which could be complemented by hydrogen-bonding in the case of benzoic acid (**2**) and 3-methyl-catechol (**6**).

It is noteworthy that **1 a** and **1 b** are aromatic molecules, where benzene linkers are connected by oxygen-bridges. The oxygen atoms in the linkages bear free electron pairs that can be conjugated with the aromatic moieties in the macrocycle, making the aromatic groups electron-rich. The calculated molecular electrostatic potential (MEP) images for **1 a** and **1 b** show that the edges of the aromatic linkers are electron-rich and the center of the aromatic linkers is electron-deficient (Figure 1b). Systems of this kind could form off-center or T-shaped π-π interactions with other aromatic species[31] as well as serve as hydrogen-bond acceptors through the oxygen-linkages.

The first complexation experiments in this work were performed between **1 a** and the electron-deficient guest molecule **2**, which carries functional groups that allow for hydrogen-bonding and π-π interactions. Two sets of NMR titration experiments were carried out in this work, at 4.5 mM and 45 mM concentrations of **1 a** in $CDCl_3$, which both indicated weak binding with the guest species (Figure 5a), however, the binding was not sufficiently strong to reach the data points with the binding probability between 0.2 and 0.8,[32,33] and therefore the association constant values reported in the SI are meant to serve as estimations.

We next undertook an NMR titration experiment with trifluoroacetic acid (TFA) to probe NMR shift changes of **1 a** by the change of the acidity of the media. TFA is a stronger acid (pK_a = 0.23)[34] than **2** (pK_a = 4.20).[35] Therefore, if NMR shift changes would be induced by the acidity of the media, one would expect pronounced changes in **1a** signals. Contrary to that, a negligible change in the shifts of H_5 and H_4 and an upfield shift of H_2 in **1 a** upon addition of TFA was observed (Figure 5b). Downfield shifts of all host hydrogens upon binding of **2** (Figure 5a) show that interaction with benzoic acid has different character compared to acidic non-aromatic guest molecules. Since TFA is a non-aromatic acid, π-π interactions for complexation are excluded for both these molecules, which allows us to conclude that π-π interactions have a key contribution to binding between **1 a** and **2** and that the

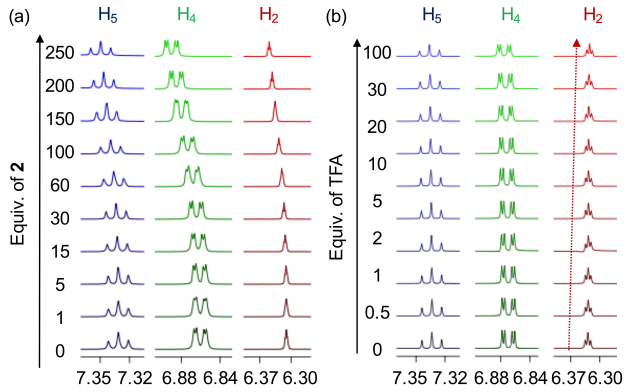

Figure 5. Evolution of proton resonances of a 45 mM solution of **1 a** in $CDCl_3$ at 288 K upon a) addition of up to 250 equivalents of **2** and b) addition of up to 100 equivalents of TFA. The three aromatic proton resonances are shown separately. Upon addition of **2**, all proton resonances shift downfield, whereas upon addition of TFA, an upfield change of chemical shift is observed for H_2 proton resonance.

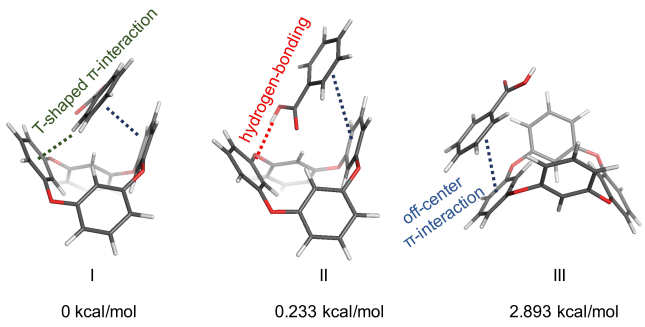

Figure 6. The three complexation geometries calculated with DFT calculations in this work. The lowest-energy complexation geometry is without any hydrogen-bonding interactions.

changes in the spectra we have observed are not induced by changes in the pH of the solution.[36]

Further insight into the possible dominant interactions for complexation was given by DFT calculations. Zuo et al. have calculated the structures and conformational energies for a series of calixarenes,[37] including oxacalix[4]arene studied in this work. Their choice of the B3LYP functional was in part made because the macrocycle was considered too constrained for the aromatic groups to undergo π-π stacking; the main source of deficiency in this functional. Our choice of the functional M06-2X[38] was primarily made based on its ability to take into account the dispersion effects of π-electron density around aromatic rings because of their importance in the complex formation[39] between **1 a** and the guest molecule **2**.

Our conformational analysis of **1 a** yielded two low energy conformers (structures shown in Figure S19). The lowest energy structure was similar to the crystal structure. We next investigated the potential interactions between the lowest energy geometry of **1 a** and **2**. The choice of initial geometries for complexation between **1 a** and **2** was based on a T-shaped π-π interaction, an off-center π-π interaction and hydrogen-bonding. Three binding geometries gave either one or more of these weak supramolecular interactions (Figure 6). In the lowest energy geometry, benzoic acid made one T-shaped and one off-center π-π interaction with phenyl groups in **1 a**. Binding geometry II was 0.233 kcal/mol higher in energy and also allowed for the formation of a hydrogen bond between the carboxylic hydrogen and the ether oxygen (2.008 Å), while geometry III relied on one off-center π-π interaction and was 2.898 kcal/mol higher in energy than binding geometry I. Even different orientations of the carboxyl group did not allow for hydrogen bonding in this structure (see SI for details). Moreover, we aimed to calculate a fourth binding geometry that forms just one hydrogen bond between **1 a** and **2**, however, this structure converted into conformation III in the course of the geometry optimization. It is noted here that these computational results serve as an estimation for interactions for complexation between **1a** and **2** as the binding demonstrated by NMR titration experiments was very weak in methanol-d_4.

Shimizu and coworkers showed ferrocene to complex with nitro-substituted oxacalix[4]arenes,[40] which led to our interest whether complexation could be detected with unsubstituted oxacalix[4]arene. The NMR titration results of **1 a** and guest **3** showed weak binding (see SI for details). Intriguingly, the peak arising from guest molecule **3** near 4.2 ppm shifted upfield when up to 5 equivalents of the guest was added, followed by downfield shifts thereafter, which could indicate aggregation of the guest species **3** during the titration experiment.

We also observed, albeit weak, complexation of **1 a** with 1,5-dimethylnaphthalene (**4**) and neocuproine (**5**) in $CDCl_3$ and 3-methylcatechol **(6)** in toluene-d_8. Even though guest species **4**, **5** and **6** showed binding with **1 a**, association constant determination was set aside due to the poor solubility of **4**, **5** and **6** in these solvents. The spectra for complexation and the respective changes in chemical shifts for **1 a** with **4**, **5**, and **6** are brought in SI. Moreover, calix[*n*]arene derivatives have been shown to complex with fullerene C_{60} (**7**) in toluene-d_8,[41,42] however, the oxacalix[*n*]arenes **1 a** and **1 b** did not show complexation based on the ^1H or ^{13}CNMR spectra for a 2:1 molar mixture of the host and the guest species **7**, which could arise from the competitive π-π interactions of **1 a** with the solvent.

The guest species **2** and **3** were selected to probe complexation with oxacalix[8]arene **1 b.** Addition of 100 equivalents of either **2** or **3** showed almost undetectable changes in chemical shifts between the host and the guest molecules (see Table S4). This is likely to arise from a size mismatch between the cavity of **1b** and the guest molecules or the more flexible nature of the larger host compound.

Conclusions

In conclusion, the interactions governing the packing of the oxacalix[*n*]arene ($n = 4$ and 8) macrocycles in their unprecedented solid state structures are characterized. Our solution state conformational study coincides with previous reports for

substituted oxacalix[4]arenes and does not allow to differentiate whether the macrocycles are in fast conformational exchange or in a static conformation in solution. NMR titration experiments with benzoic acid and ferrocene show weak complexation at room temperature. The oxacalix[8]arene host does not show detectable complexation in solution with ferrocene and benzoic acid, which is attributed to their size mismatch or the more flexible nature of the host.

Supporting Information Summary

Detailed experimental section, details of analysis of interaction energies in the crystal structures, variable temperature NMR spectra, NMR spectra for compounds **1a** and **1b** with and without guest species **2**-**7**, NMR titration experiments results and further DFT calculation details.

Acknowledgements

This research was supported by the Estonian Ministry of Education and Research through Grants MOBJD39, IUT23-7 and PUT692 and the EU European Regional Development Fund through grant TK134. We would like to acknowledge Kari Rissanen for help with the manuscript.

Conflict of Interest

The authors declare no conflict of interest.

Keywords: conformational study · host-guest complexation · oxacalix[*n*]arene · NMR titration · nuclear magnetic resonance · single crystal structure

[1] C. J. Pedersen, *Angew. Chemie Int. Ed. English* **1988**, *27*, 1021–1027.
[2] M. Hiraoka, *Crown Ethers and Analogous Compounds*, Elsevier, **2016**.
[3] G. Crini, *Chem. Rev* **2014**, *114*, 10940–10975.
[4] W. A. Freeman, W. L. Mock, N. Y. Shih, *J. Am. Chem. Soc.* **1981**, *103*, 7367–7368.
[5] K. I. Assaf, W. M. Nau, *Chem. Soc. Rev.* **2015**, *44*, 394–418.
[6] M.-Z. Asfari, V. Böhmer, J. Harrowfield, J. Vicens, *Calixarenes 2001*, Springer Science & Business Media, **2007**.
[7] J. Vicens, V. Böhmer, *Calixarenes: A Versatile Class of Macrocyclic Compounds*, Springer Science & Business Media, **2012**.
[8] W. Maes, W. Dehaen, *Chem. Soc. Rev.* **2008**, *37*, 2393–2402.
[9] N. Sommer, H. A. Staab, *Tetrahedron Lett.* **1966**, *7*, 2837–2841.
[10] J. L. Katz, M. B. Feldman, R. R. Conry, *Org. Lett.* **2005**, *7*, 91–94.
[11] J. L. Katz, B. J. Geller, P. D. Foster, *Chem. Commun.* **2007**, *10*, 1026–1028.
[12] W. Van Rossom, J. Caers, K. Robeyns, L. Van Meervelt, W. Maes, W. Dehaen, *J. Org. Chem.* **2012**, *77*, 2791–2797.
[13] S. Akagi, Y. Yasukawa, K. Kobayashi, H. Konishi, *Tetrahedron* **2009**, *65*, 9983–9988.
[14] C. Capici, D. Garozzo, G. Gattuso, A. Messina, A. Notti, M. F. Parisi, I. Pisagatti, S. Pappalardo, *Ark. Online J. Org. Chem.* **2009**, *8*, 199–211.
[15] R. D. Chambers, P. R. Hoskin, A. Khalil, P. Richmond, G. Sandford, D. S. Yufit, J. A. K. Howard, *J. Fluor. Chem.* **2002**, *116*, 19–22.
[16] W. Van Rossom, K. Robeyns, M. Ovaere, L. Van Meervelt, W. Dehaen, W. Maes, *Org. Lett.* **2010**, *13*, 126–129.
[17] W. Van Rossom, M. Ovaere, L. Van Meervelt, W. Dehaen, W. Maes, *Org. Lett.* **2009**, *11*, 1681–1684.
[18] D. Sobransingh, M. B. Dewal, J. Hiller, M. D. Smith, L. S. Shimizu, *New J. Chem.* **2008**, *32*, 24–27.
[19] N. Manganaro, G. Lando, C. Gargiulli, I. Pisagatti, A. Notti, S. Pappalardo, M. F. Parisi, G. Gattuso, *Chem. Commun.* **2015**, *51*, 12657–12660.
[20] N. Manganaro, G. Lando, I. Pisagatti, A. Notti, S. Pappalardo, M. F. Parisi, G. Gattuso, *Supramol. Chem.* **2016**, *28*, 493–498.
[21] J. E. McMurry, J. C. Phelan, *Tetrahedron Lett.* **1991**, *32*, 5655–5658.
[22] F. Grynszpan, S. E. Biali, *Tetrahedron Lett.* **1991**, *32*, 5155–5158.
[23] F. Inokuchi, Y. Miyahara, T. Inazu, S. Shinkai, *Angew. Chemie Int. Ed.* **1995**, *34*, 1364–1366.
[24] Q. Zhou, L. Su, T. Jiang, B. Zhang, R. Chen, H. Jiang, Y. Ye, M. Zhu, D. Han, J. Shen, et al., *Tetrahedron* **2014**, *70*, 1125–1132.
[25] M. J. Turner, S. Grabowsky, D. Jayatilaka, M. A. Spackman, *J. Phys. Chem. Lett.* **2014**, *5*, 4249–4255.
[26] C. F. Mackenzie, P. R. Spackman, D. Jayatilaka, M. A. Spackman, *IUCrJ* **2017**, *4*, 575-587.
[27] J. J. McKinnon, M. J. Turner, D. Jayatilaka, M. A. Spackman, D. J. Grimwood, S. K. Wolff, *Univ. West. Aust.* **2012**.
[28] C. R. Martinez, B. L. Iverson, *Chem. Sci.* **2012**, *3*, 2191–2201.
[29] R. D. Chambers, P. R. Hoskin, A. R. Kenwright, A. Khalil, P. Richmond, G. Sandford, D. S. Yufit, J. A. K. Howard, *Org. Biomol. Chem.* **2003**, *1*, 2137–2147.
[30] M.-X. Wang, H.-B. Yang, *J. Am. Chem. Soc.* **2004**, *126*, 15412–15422.
[31] C. R. Martinez, B. L. Iverson, *Chem. Sci.* **2012**, *3*, 2191–2201.
[32] P. Thordarson, *Chem. Soc. Rev.* **2011**, *40*, 1305–1323.
[33] C. S. Wilcox, *Front. Supramol. Org. Chem. Photochem.* **1991**, *123-143*.
[34] J. B. Milne, T. J. Parker, *J. Solution Chem.* **1981**, *10*, 479–487.
[35] D. C. Harris, *Quantitative Chemical Analysis*, Macmillan, **2010**.
[36] Katz et al. reported in their study in Ref. [11] that benzoic acid causes small upfield shifts (<0.05 ppm) in the resonances of oxacalix[4]naphthalene[2]naphthyridine, whereas downfield shifts are observed in this study. The analysis of this discrepancy is beyond the scope of this work, though worth highlighting in itself.
[37] C. Zuo, O. Wiest, Y. Wu, *J. Phys. Org. Chem.* **2011**, *24*, 1157–1165.
[38] Y. Zhao, D. G. Truhlar, *Theor. Chem. Acc.* **2008**, *120*, 215–241.
[39] E. G. Hohenstein, S. T. Chill, C. D. Sherrill, *J. Chem. Theory Comput.* **2008**, *4*, 1996–2000.
[40] D. Sobransingh, M. B. Dewal, J. Hiller, M. D. Smith, L. S. Shimizu, *New J. Chem.* **2008**, *32*, 24–27.
[41] J. L. Atwood, G. A. Koutsantonis, C. L. Raston, *Nature* **1994**, *368*, 229–231.
[42] S. Mizyed, M. Ashram, D. O. Miller, P. E. Georghiou, *J. Chem. Soc. Perkin Trans. 2* **2001**, 1916–1919.

Submitted: May 25, 2018
Accepted: July 9, 2018